Macromolecules

pubs.acs.org/Macromolecules Article

Synthesis of Self-Healing Elastomers by Scandium-Catalyzed Terpolymerization of Ethylene, Styrene, and Dimethylaminophenyl-Substituted Propylene

Haoran Zhang,[#] Lin Huang,[#] Xia Wu, Mingjun Chi, Haobing Wang, Masayoshi Nishiura,* Yuji Higaki, Tetsuro Murahashi, and Zhaomin Hou*

Cite This: *Macromolecules* 2024, 57, 7219−7226 Read Online

ACCESS | Metrics & More | Article Recommendations | Supporting Information

ABSTRACT: The synthesis of self-healing polymers by catalyst-controlled copolymerization of commodity olefins is of fundamental interest and practical importance but remains highly challenging. We report here the synthesis of a new family of self-healing elastomers through terpolymerization of ethylene (**E**), styrene (**St**), and dimethylaminophenyl-substituted propylene (**AMP**) using a sterically demanding half-sandwich scandium catalyst. The terpolymers, comprising **AMP**−*alt*−(**E**−**E**) sequences and **St**−**St** and **E**−**E** blocks, exhibited excellent elasticity and rapid self-healing properties. Notably, employing 4-*tert*-butylstyrene instead of unsubstituted styrene in the terpolymerization yielded the corresponding terpolymers with further enhanced mechanical strength and self-healing capabilities. X-ray diffraction analyses and scanning transmission electron microscopy (STEM) images of an **E**−**St**−**AMP** terpolymer revealed a nanophase-separated structure comprising crystalline **E**−**E** and glassy amorphous **St**−**St** nanodomains dispersed in a rubbery **AMP**−**E**−**E** matrix, providing insights into its remarkable mechanical and self-healing properties. This work represents a significant advancement in the synthesis of olefin-based self-healing polymers with potential applications in various fields.

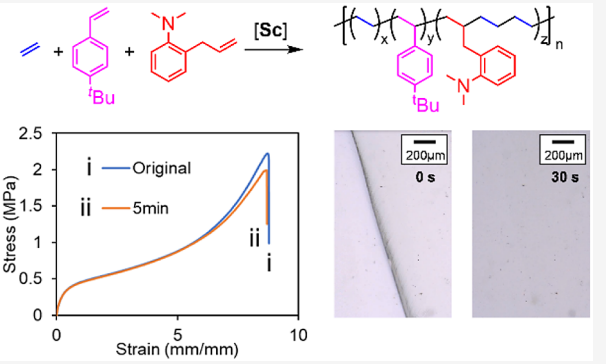

INTRODUCTION

Polymers capable of autonomously repairing mechanical damage have garnered significant attention over the past decades due to their potential to enhance durability, safety, and environmental sustainability across various applications.[1−4] Most self-healing polymers reported so far mainly rely on reversible covalent bond formation (such as Diels−Alder reactions) and supramolecular interactions (such as hydrogen bonds and ion pair interactions),[3,4] while self-healing polymers based on van der Waals force remain relatively underexplored.[5−13] Polyolefins are widely used in modern society ranging from food packaging to automobiles, electronics, and medical devices.[14−17] Integrating self-healing properties into olefin-based polymers could improve the lifetime and safety of many products, reduce plastic disposal, and alleviate environment pollution. However, despite considerable interest and extensive studies in self-healing materials, olefin-based self-healing polymers have been scarcely explored, possibly due to challenges in embedding suitable self-healing mechanisms into polyolefins.

In 2012, Guan and coworkers reported the synthesis of a self-healing thermoplastic elastomer by introducing amide-containing polyacrylate brushes into a polystyrene backbone constructed through radical polymerization.[18] In this system, hydrogen-bonding interactions of the amide units in the polymer brushes played a crucial role in achieving self-healing. In 2020, Chen and coworkers prepared self-healing polyolefins based on ion-pair interactions by introducing metal ions (such as Fe^{3+}) into carboxylic acid or catechol side arms in a polyolefin backbone synthesized through palladium-catalyzed terpolymerization.[19,20] More recently, Urban and coworkers found that styrene-based polymers comprising primarily alternating styrene-*n*-butyl acrylate sequences synthesized through radical polymerization could autonomously self-heal via interchain interactions between the *n*-butyl side groups and phenyl rings without relying on chemical interactions.[11] Li and coworkers found that polyolefins obtained by hydrogenation of syndiotactic poly(methoxyphenylbutadienes) could also exhibit self-healability through interchain interactions between

Received: April 11, 2024
Revised: June 25, 2024
Accepted: June 28, 2024
Published: July 16, 2024

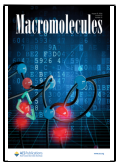

https://doi.org/10.1021/acs.macromol.4c00819
Macromolecules 2024, 57, 7219−7226

Table 1. Scandium-Catalyzed Terpolymerization of Ethylene (E), styrene (St), and 3-(*o*-Dimethylaminophenyl)propylene (AMP)[a]

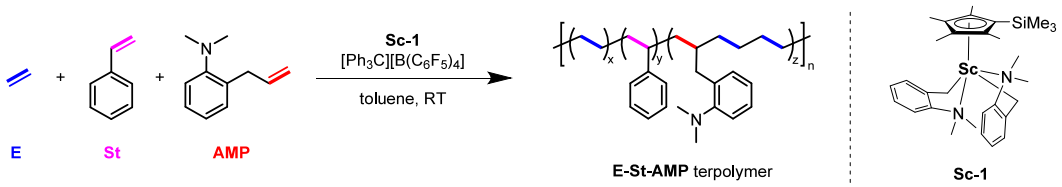

run	[St]/[AMP]/[Sc]	time	yield (g)[b]	St conv (%)	AMP conv (%)	M_n ($\times 10^3$g mol^{-1})[c]	M_w/M_n[c]	E/St/AMP(mol %)[d]	T_g/T_m (°C)[e]
1	250:250:1	45 min	1.56	30	97	66 (**P1**)	1.9	72/7/21	−23/124
2	500:500:1	80 min	3.18	48	98	116 (**P2**)	1.8	73/9/18	−23/125
3[f]	1000:1000:1	4 h	5.52	41	90	131 (**P3**)	1.8	72/8/20	−20/121
4	1000:500: 1	70 min	2.72	25	88	107 (**P4**)	1.8	65/14/21	−17/125
5	1500:500: 1	80 min	3.38	32	93	98 (**P5**)	1.6	60/21/19	−14/124
6	2000:500: 1	90 min	4.30	48	78	110 (**P6**)	1.6	57/32/11	−11/219

[a]Conditions unless otherwise noted: [**Sc-1**] (0.02 mmol), [Ph_3C][$B(C_6F_5)_4$] (0.02 mmol), ethylene (1 atm), 25 mL toluene. [b]Yield of polymer. [c]Determined by high temperature GPC in 1,2-dichlorobenzene at 145 °C against polystyrene standard. [d]Incorporation ratio of comonomer. [e]Determined by differential scanning calorimetry (DSC). [f]50 mL toluene.

the methoxyphenyl side groups via van der Waals forces enhanced by dipole−dipole interaction.[12]

Our group has been engaged in regio- and stereocontrolled polymerization and copolymerization of various olefins by using organo rare-earth catalysts.[21−23] In our recent studies on the copolymerization of nonpolar and polar olefins,[6,7,13,24−26] we found that the copolymerization of ethylene and anisyl-substituted propylenes using a sterically demanding half-sandwich scandium catalyst afforded unique multiblock copolymers composed of relatively long ethylene−*alt*−anisylpropylene sequences and short ethylene−ethylene blocks. Such sequence-regulated copolymers could autonomously self-heal under various chemical environments through microphase separation of crystalline ethylene−ethylene nanodomains from a flexible ethylene−*alt*−anisylpropylene matrix via van der Waals interactions.[6,7,13] The key to success in making these sequence-regulated copolymers was the unique interaction between the oxygen atom in an anisylpropylene monomer and the scandium atom in the catalyst. These results raised an intriguing question of whether self-healing polyolefins with other heteroatom functional groups could be synthesized analogously. Given widespread interest in amine-functionalized polymers[27,28] and the circulation of commodity polyolefins,[14−17] we then examined the copolymerization of dimethylaminophenyl-functionalized propylene with ethylene and styrene. In this article, we report the terpolymerization of ethylene (**E**), styrene (**St**), and 3-(*o*-dimethylaminophenyl)-propylene (**AMP**) by a sterically demanding half-sandwich scandium catalyst. We found that the terpolymerization took place in a sequence-controlled fashion, affording the terpolymer products comprising **AMP**−*alt*−(**E**−**E**) sequences and **St**−**St** and **E**−**E** blocks. The terpolymers exhibited excellent elasticity and rapid self-healing properties, standing in contrast with the corresponding binary copolymers, none of which were self-healable. Moreover, the use of 4-*tert*-butylstyrene instead of unsubstituted styrene in the terpolymerization afforded the corresponding terpolymers with further enhanced mechanical strength and self-healing capabilities. X-ray diffraction analyses and scanning transmission electron microscopy (STEM) images of an **E**−**St**−**AMP** terpolymer revealed a nanophase-separated structure comprising crystalline **E**−**E** and glassy amorphous **St**−**St** nanodomains dispersed in a rubbery **AMP**−**E**−**E** matrix, providing insights into its remarkable mechanical and self-healing properties.

RESULTS AND DISCUSSION

As reported previously,[29] the binary copolymerization of ethylene and styrene by the $C_5Me_4SiMe_3$-ligated half-sandwich scandium catalyst $(C_5Me_4SiMe_3)Sc(CH_2C_6H_4NMe_2\text{-}o)_2$ (**Sc-1**) in combination with [Ph_3C][$B(C_6F_5)_4$] afforded a multiblock **E**−**St** copolymer behaving as hard plastic with T_g = 63 °C and T_m = 234 °C (Figure S1). The copolymerization of styrene with 3-(*o*-dimethylaminophenyl)propylene (**AMP**) by **Sc-1**/[Ph_3C][$B(C_6F_5)_4$] yielded a white powdery polymer product with T_g = 62 °C (Figure S2).[26] In contrast, the copolymer synthesized by the binary copolymerization of ethylene with **AMP** behaved like soft viscoelastic material showing T_g at −27 °C and T_m at 125 °C (Table S1, Run 1; Figure S4).[30,31] None of these binary copolymers showed a visible self-healing behavior. To see possible synergistic effects of the three different monomers on the mechanical properties of the resulting copolymers, the terpolymerization of ethylene, styrene, and **AMP** was then examined. With a feed ratio of [**St**]/[**AMP**]/[**Sc**] = 250/250/1 under 1 atm of ethylene, the terpolymerization smoothly took place at room temperature, yielding an **E**−**St**−**AMP** terpolymer (**P1**) with $M_n = 66 \times 10^3$ g mol^{-1} (M_w/M_n = 1.9) and a comonomer incorporation ratio **E**/**St**/**AMP** = 72/7/21 (Table 1, Run 1).[30,32] Raising the monomer to catalyst feed ratio [**St**]/[**AMP**]/[**Sc**] from 250/250/1 to 500/500/1 and 1000/1000/1 afforded higher molecular weight polymers (**P2**: $M_n = 116 \times 10^3$ g mol^{-1} and **P3**: 131×10^3 g mol^{-1}, respectively) with the similar **E**/**St**/**AMP** incorporation ratios (73/9/18 and 72/8/20, respectively) (Table 1, Runs 2 and 3). With [**AMP**]/[**Sc**] = 500/1, raising the styrene feed per catalyst from 500 equiv to 1000, 1500, and 2000 equiv resulted in the increase of the **St** content in the terpolymers from 9 mol % (**P2**) to 14 mol % (**P4**), 21 mol % (**P5**), and 32 mol % (**P6**), respectively (Table 1, Runs 2, 4−6).

The microstructures of the **E**−**St**−**AMP** terpolymers were thoroughly characterized by the NMR analyses (see Supporting Information for details). Methine and methylene carbons were distinguished by the DEPT analyses. Direct ^1H−^{13}C correlations were established by HSQC and HETCOR spectral

https://doi.org/10.1021/acs.macromol.4c00819
Macromolecules 2024, 57, 7219−7226

data. Correlations around methine carbons were assigned by HMBC analyses. HMBC cross-peaks from aromatic protons with benzyl carbons were used to assign styrene and **AMP** units. Relatively weak signals were carefully assigned by comparison of spectral data with those of the corresponding binary copolymers. The comonomer incorporation ratios were calculated based on the integration of the ^{1}H NMR signals. It was revealed that the terpolymers obtained in this work possessed sequence-controlled multiblock microstructures comprising **AMP**−*alt*−(**E**−**E**) segments and short **St**−**St** and **E**−**E** blocks. The ^{1}H NMR spectrum and the aliphatic part of the ^{13}C{^{1}H} NMR spectrum of a typical **E**−**St**−**AMP** terpolymer **P5** (obtained in Table 1, Run 5) are shown in Figure 1a,b, respectively. The signals appearing around 43.4

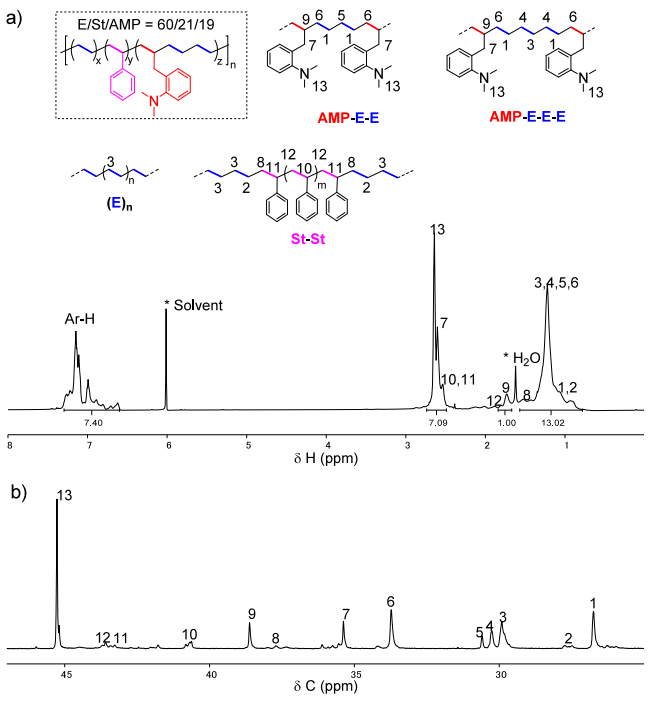

Figure 1. a) ^{1}H NMR spectrum of **E**−**St**−**AMP** terpolymer **P5** (Table 1, Run 5) in $C_2D_2Cl_4$. b) Aliphatic part of the ^{13}C{^{1}H} NMR spectrum of **P5** in $C_2D_2Cl_4$.

(C12), 43.0 (C11), and 40.4 (C10) in the ^{13}C{^{1}H} NMR spectrum could be assigned to the continuous **St**-**St** units (Figure 1b), while the **E**-**St**-**E** units were almost negligible, in agreement with what was observed in the two-component copolymerization of ethylene and styrene (Figure S14).[29] The ^{13}C{^{1}H} NMR signals at 33.5 (C6), 30.4 (C5), 30.0 (C4), 29.7 (C3), and 26.5 (C1) ppm could be assigned to **AMP**-**E**-**E**, **AMP**-**E**-**E**-**E**, and **E**-**E** sequences by comparison with the ^{13}C{^{1}H} NMR spectrum of the two-component **E**-**AMP** copolymer (Figure S23). Continuous **AMP**−**AMP** units, **AMP**−*alt*−**E** units, and **AMP**−*alt*−**St** units were not observed probably owing to the steric hindrance of the NMe_2 group in **AMP**.[33]

Terpolymers **P1**−**P6** showed glass transition temperatures (T_g) in a range of −23 °C to −11 °C, generally rising as the styrene content was increased (Table 1). Terpolymers with styrene content below 21 mol % (**P1**−**P5**) exhibited melting points (T_m) originated from the polyethylene units (121−125 °C) (Table 1, Runs 1−5), while a polymer (**P6**) having higher styrene content (32 mol %) showed a T_m at 219 °C possibly originating from syndiotactic **St**−**St** sequences (Table 1, Run 6).[29,34−37]

The mechanical properties of the terpolymers with different molecular weights and comonomer ratios are shown in Figure 2 (see also Figures S5−S9). Terpolymer **P1** with a relatively low M_n (66×10^3 g mol^{-1}) containing 7 mol % **St** behaved like a soft viscoelastic material (Figure 2b). In contrast, the higher molecular polymers **P2** ($M_n = 116 \times 10^3$) and **P3** (131×10^3 g mol^{-1}) with a similar **St** content (8−9 mol %) exhibited the typical features of elastomer (Video S1), showing higher toughness as the molecular weight became larger (Figure 2a,b). The more incorporation of styrene resulted in a more pronounced enhancement of the mechanical strength, surpassing the influence of increase of molecular weight. As the styrene content increased from 9 mol % (**P2**, $M_n = 116 \times 10^3$) to 14 mol % (**P4**, $M_n = 107 \times 10^3$) and 21 mol % (**P5**, $M_n = 98 \times 10^3$), the tensile strength of the terpolymers rose from 1.3 to 1.9 and 4.4 MPa, respectively, with elongation at break higher than 1200%. Terpolymer **P6** with a styrene content of 30 mol % behaved like a flexible plastic at room temperature, showing a tensile strength of 12.7 MPa with 390% elongation at break. In addition to excellent elasticity and toughness, **P2**−**P5** showed remarkable self-healing properties (Video S2). When a thin film of **P2** was cut into two pieces and then brought together at room temperature, rapid repairing was observed. After only 5 min, the repaired film could be stretched to 1100%. The fracture was almost completely mended in 1 h as evidenced by an elongation similar to that of the original sample (Figure 2c). In the case of **P5**, a self-healed sample showed a tensile strength as high as 4.3 MPa with 1350% elongation at break after repaired in 2 days (Figure 2d, v).

To further investigate the influence of styrene units on the mechanical properties of the terpolymers, the copolymerization of 4-substituted styrenes with ethylene and **AMP** was examined. Under the same conditions, 4-methylstyrene (**MeSt**) showed a higher activity than that of unsubstituted styrene probably due to the electron-donating influence of the alkyl substituents. With a feed ratio of [**MeSt**]/[**AMP**]/[**Sc**] = 250/250/1 under 1 atm of ethylene (**E**), a terpolymer with $M_n = 68 \times 10^3$ g mol^{-1} and a commoner incorporation ratio of **E**/**MeSt**/**AMP** = 71/15/14 was obtained (Table 2, Run 1). 4-*tert*-Buytlstyrene (**^{t}BuSt**) exhibited a further higher activity. The terpolymerization of ethylene (**E**), **^{t}BuSt**, and **AMP** with monomer-to-catalyst ratio [**^{t}BuSt**]/[**AMP**]/[**Sc**] = 125/250/1 under 1 atm of ethylene yielded a terpolymer (**P7**) with $M_n = 63 \times 10^3$ g mol^{-1} and commoner incorporation ratio **E**/**^{t}BuSt**/**AMP** = 67/16/17 (Table 2, Run 2). Raising the **^{t}BuSt** feed per catalyst from 125 equiv to 250 and 375 equiv resulted in an elevation of the **^{t}BuSt** content in the terpolymer products from 16 mol % (**P7**) to 20 mol % (**P8**) and 27 mol % (**P9**), respectively (Table 2, Runs 2−4). Elevating the monomer-to-catalyst ratio [**^{t}BuSt**]/[**AMP**]/[**Sc**] from 250/250/1 to 500/500/1 resulted in a rise of the polymer molecular weight from $M_n = 60 \times 10^3$ g mol^{-1} (**P8**) to $M_n = 124 \times 10^3$ g mol^{-1} (**P10**), with the **^{t}BuSt**/**E**/**AMP** incorporation ratio remaining almost unchanged (65/20/15 vs 62/22/16) (Table 2, Runs 3 and 5).

The **MeSt**-containing terpolymer showed similar mechanical properties to those of the unsubstituted styrene-containing analogues (see Figure S10). In contrast, the mechanical properties of the **E**−**^{t}BuSt**−**AMP** terpolymers **P7**−**P10** are shown in Figure 3. The terpolymer **P7** with a **^{t}BuSt** content of 16 mol % showed a tensile strength of 2.2 MPa with 890% elongation at break (Figure 3a and 3b). An almost complete

https://doi.org/10.1021/acs.macromol.4c00819
Macromolecules 2024, 57, 7219−7226

a

Polymer	E/St/AMP	M_n (kDa)	Initial Modulus (MPa)	Elongation at Break (%)	Ultimate Tensile Strength (MPa)	Toughness (10^6 J/m^3)	Type of Materials
P1	72/7/21	66	1.1 ± 0.1	> 5000	0.6 ± 0.1	-	Stress softening
P2	73/9/18	116	1.3 ± 0.1	1350 ± 95	1.3 ± 0.2	11.0 ± 2.1	Elastomer
P3	72/8/20	131	2.2 ± 0.2	1300 ± 70	1.7 ± 0.2	14.1 ± 1.9	Elastomer
P4	65/14/21	107	3.7 ± 0.6	1240 ± 66	1.9 ± 0.2	17.2 ± 2.9	Elastomer
P5	60/21/19	98	4.3 ± 0.9	1400 ± 73	4.4 ±0.4	34.8 ± 4.2	Elastomer
P6	57/32/11	110	41.0 ± 5.5	390 ± 23	12.7 ± 1.8	35.3 ± 6.8	Flexible plastic

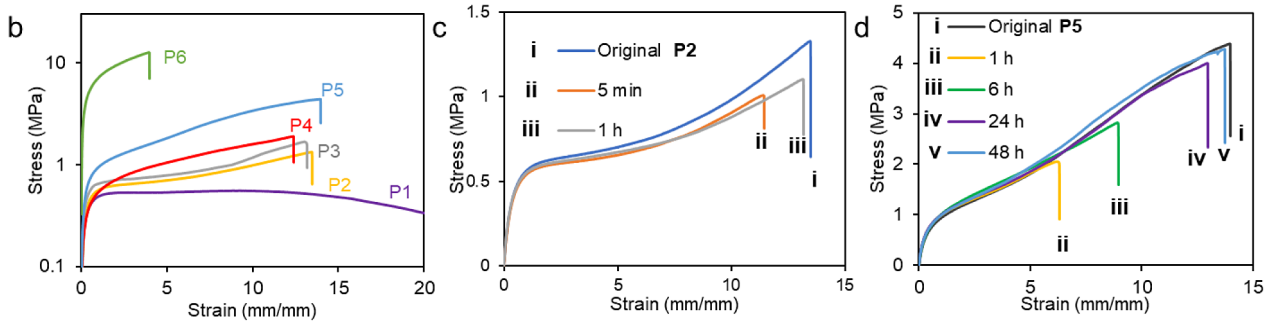

Figure 2. Mechanical properties of terpolymers with different molecular weight and monomer contents. a) Tabular summary of mechanical properties of **P1**−**P6**. b) Strain−stress curves of **P1**−**P6**. c) Self-healing tests of **P2** in air at 25 °C. d) Self-healing tests of **P5** in air at 25 °C.

Table 2. Scandium-Catalyzed Terpolymerization of Ethylene (E), Substituted styrenes (RSt), and 3-(*o*-Dimethylaminophenyl)propylene (AMP)[a]

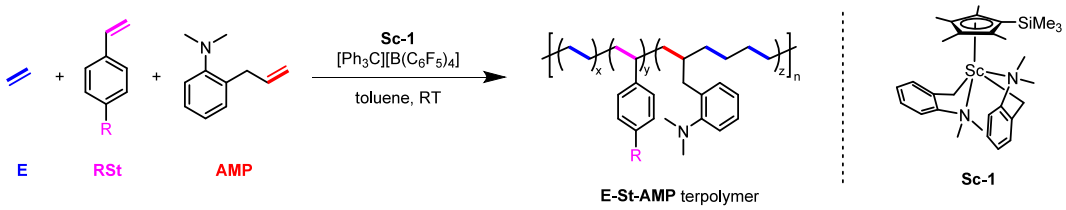

run	R	[RSt]/[AMP]/[Sc]	time (min)	yield (g)[b]	RSt conv (%)	AMP conv (%)	M_n ($\times 10^3$g mol^{-1})[c]	M_w/M_n[c]	E/RSt/AMP (mol %)[d]	T_g/T_m (°C)[e]
1	Me	250:250:1	60	1.89	92	86	68	2.0	71/15/14	−12/124
2	^{t}Bu	125:250:1	45	1.21	99	56	63 (**P7**)	2.2	67/16/17	−11/125
3	^{t}Bu	250:250:1	45	1.90	99	79	60 (**P8**)	2.0	65/20/15	−11/124
4	^{t}Bu	375:250:1	30	2.23	95	78	95 (**P9**)	2.4	59/27/14	3/125
5	^{t}Bu	500:500:1	90	3.20	85	68	124 (**P10**)	2.0	62/22/16	−5/124

[a]Conditions unless otherwise noted: [Sc] (0.02 mmol), [Ph_3C][$B(C_6F_5)_4$] (0.02 mmol), ethylene (1 atm), 25 mL toluene. [b]Yield of polymer. [c]Determined by high temperature GPC in 1,2-dichlorobenzene at 145 °C against polystyrene standard. [d]Incorporation ratio of comonomer. [e]Determined by differential scanning calorimetry (DSC).

repair was observed after the two cut pieces were put together at room temperature for 5 min (Figure 3c). A scratch made by a razor autonomously self-healed (disappeared) within 30 s (Figure 3d, Video S3). Remarkably, the self-healing rapidly took place not only in air but also in water, seawater, and alkaline (1 M NaOH) and acidic (1 M HCl) environments (Figure 3e). The terpolymer **P8** with ^{t}**BuSt** content = 20 mol % and $M_n = 60 \times 10^3$ g mol^{-1} exhibited a tensile strength of 3.9 MPa, and a cut sample completely repaired within 1 h (Figure 3f). The higher molecular-weight polymer **P10** (^{t}**BuSt** content = 22 mol %, $M_n = 124 \times 10^3$ g mol^{-1}) exhibited a tensile strength as high as 6.2 MPa with 810% elongation at break, and a self-healed sample showed a tensile strength of 6.0 MPa after 12 h repairing (Figure 3g). These terpolymers are among the toughest and fastest autonomous self-healing polymers reported so far in the literature.[7,13]

To gain information on the phase separation of the terpolymers, we conducted the wide-angle X-ray diffraction (WAXD) and small-angle X-ray scattering (SAXS) analyses of **P2** (Figure 4). The diffraction peaks at $q = 15.26$ nm^{-1} could be identified to the (110) lattice plane of the orthorhombic polyethylene crystallites generated by the **E**−**E** sequences. The crystallinity (0.28%) was evaluated by comparison of the peak area of amorphous and crystalline units (Figure 4a). Extremely diffuse scattering was observed over $q = 0.2$−0.3 nm^{-1} in the SAXS profile (Figure 4b), indicating the presence of electron density inhomogeneity. It is presumed that there exists a phase-separated structure without the lattice order. The statistical mean long period (L) and domain diameter (d) for the disordered phase-separated structure were determined to be 26 and 5.8 nm, respectively, by autocorrelation function analysis (Figure 4c). The periodic microphase separated structure would consist of **E**−**E** fine crystallites and glassy amorphous **St**−**St** nanodomains dispersed in a rubbery **AMP**−**E**−**E** matrix (Figure 5). The scanning transmission electron microscopy (STEM) images of **P2** exhibited multiphase

https://doi.org/10.1021/acs.macromol.4c00819
Macromolecules 2024, 57, 7219−7226

a

Polymer	E/^{t}BuSt/AMP	M_n (kDa)	Initial Modulus (MPa)	Elongation at Break (%)	Ultimate Tensile Strength (MPa)	Toughness (10^6 J/m^3)	Type of materials
P7	67/16/17	63	2.2 ± 0.2	890 ± 50	2.2 ± 0.4	8.3 ±0.6	Elastomer
P8	65/20/15	60	8.5 ± 0.9	760 ± 32	3.9 ± 0.3	13.8 ± 1.9	Elastomer
P9	59/27/14	95	94.0 ± 6.2	420 ± 22	9.4 ± 0.9	28.7 ± 4.2	Flexible plastic
P10	62/22/16	124	12.3 ± 1.4	810 ± 39	6.2 ± 0.4	22.6 ± 2.1	Elastomer

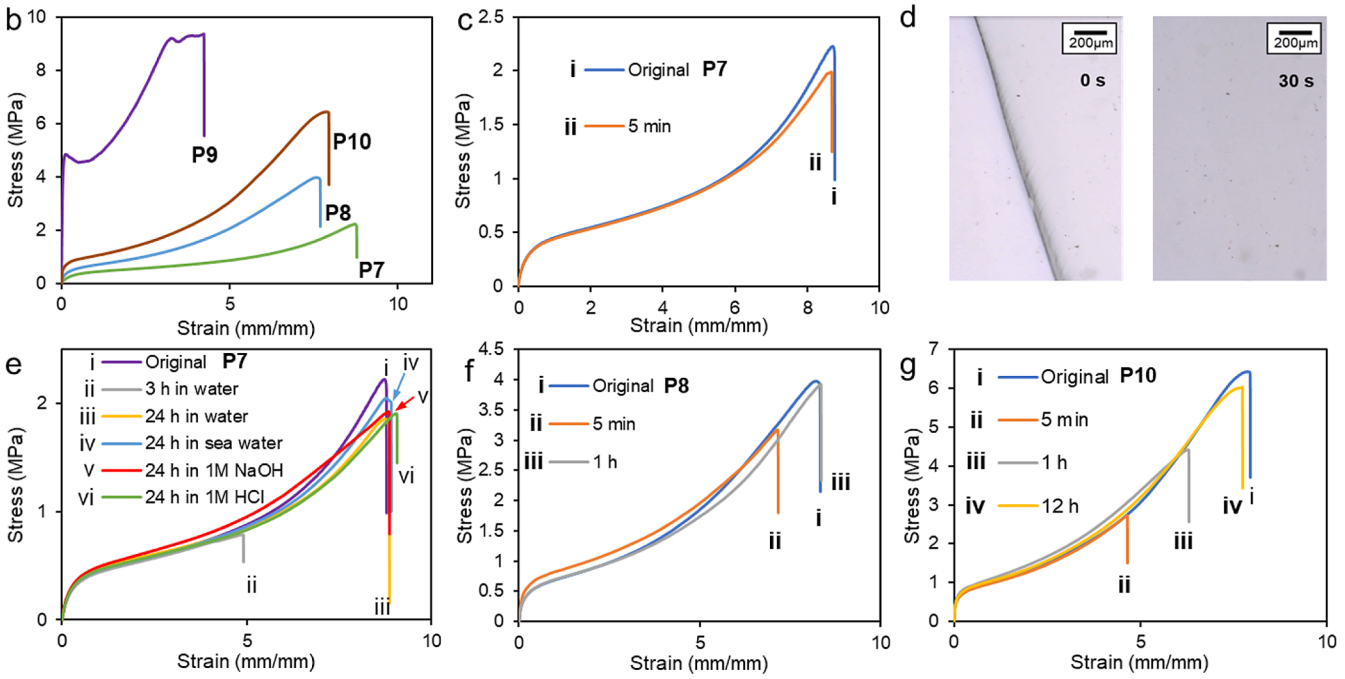

Figure 3. Mechanical properties of 4-*tert*-buytlstyrene (^{t}**BuSt**)-containing terpolymers **P7**−**P10**. a) Tabular summary of mechanical properties. b) Strain−stress curves. c) Self-healing tests of **P7** in air at 25 °C. d) Optical microscope pictures of damaged (left) and self-healed (right) samples of **P7** in air at 25 °C. A film of **P7** was scratched by a razor and then left in air for 30 s for repairing. e) Self-healing tests of **P7** in water, seawater, and aqueous acid (1 M HCl) and alkaline (1 M NaOH) solutions at 25 °C. f) Self-healing tests of terpolymer **P8** in air at 25 °C. g) Self-healing tests of terpolymer **P10** in air at 25 °C.

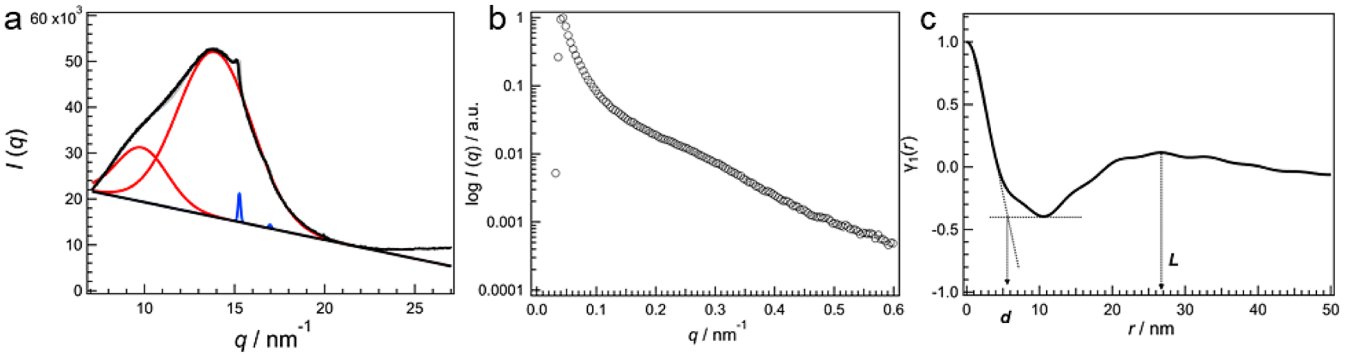

Figure 4. X-ray Diffraction analyses of terpolymer **P2**. a) Wide-angle X-ray diffraction (WAXD) analysis. b) Azimuthally averaged small-angle X-ray scattering (SAXS) intensity profile. c) Normalized one-dimensional correlation function γ(r) for the SAXS curve.

morphology at nanoscale (Figure S96), in agreement with the X-ray diffraction analyses.

In principle, polymer chain interdiffusion at temperatures above glass transition temperature (T_g) would enable a polymer to self-heal upon mechanical damage, if the mobility is sufficiently high.[1,4] In the present sequence-regulated multiblock **E-St-AMP** terpolymers, the polymer chain interactions via van der Waals force could lead to the formation of a physically cross-linked, three-dimensional network at the nanoscale through multiple-phase separation of hard nanodomains of aggregated crystalline **E**−**E** sequences and the rigid **St**−**St** segments from a highly flexible **AMP**−**E**−**E** segment matrix, thereby affording excellent elasticity (Figure 5). When mechanically damaged, the three-dimensional nano network may be restored through reaggregation of the **E**−**E** and **St**−**St** segments and re-entanglement of the flexible **AMP**−**E**−**E** segments. The rapid self-healing and remarkable elasticity of the terpolymers could be attributed to the formation of diversified nanodomains generated by different components. The high mobility of the soft **AMP**−**E**−**E**

https://doi.org/10.1021/acs.macromol.4c00819
Macromolecules 2024, 57, 7219−7226

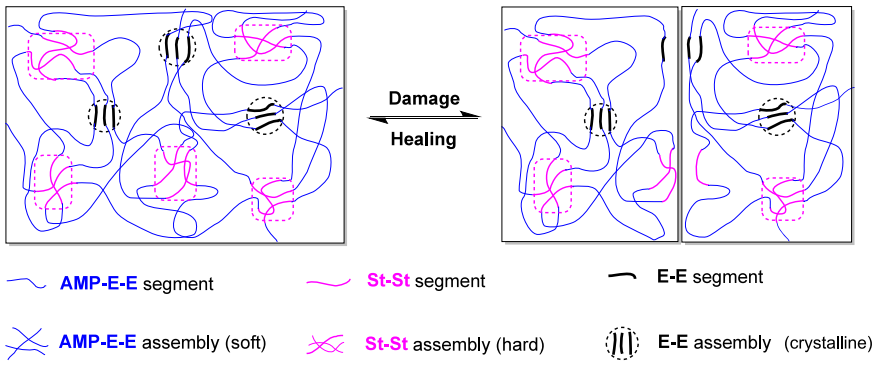

Figure 5. Plausible self-healing mechanism of an **E**−**St**−**AMP** terpolymer.

segments may facilitate rapid recovery of the **E**−**E** crystalline nanodomains and rigid **St**−**St** nanodomains. The exhibition of both higher tensile strength and higher self-healing speed of an **E**−^{t}**BuSt**−**AMP** terpolymer compared to the **E**−**St**−**AMP** analogue might be due to the stronger cross-linking (nanodomain) formed by the ^{t}**BuSt**−^{t}**BuSt** sequences versus the **St**−**St** sequences, as well as the aggregation dynamics facilitated by the bulky ^{t}Bu group.[38,39]

CONCLUSION

In summary, we have achieved for the first time the terpolymerization of ethylene (**E**), styrene (**St**), and dimethylaminophenyl-substituted propylene (**AMP**) in a sequence-regulated fashion by using a sterically demanding half-sandwich scandium catalyst such as **Sc-1**. The resulting terpolymers (such as **P2**−**P5**) exhibited excellent elasticity and self-healability through nanophase separation of crystalline **E**−**E** and glassy **St**−**St** nanodomains from a soft **AMP**−*alt*−(**E**−**E**) matrix. The analogous 4-*tert*-butylstyrene-incorporated terpolymers (such as **P10**) exhibited further enhanced tensile strength and higher self-healing speed, showcasing significant substituent effects on the mechanical and self-healing properties of the resultant polymers. This work demonstrates that sequence-regulated copolymerization of multiple olefins with different properties may serve as an efficient route for the synthesis of novel self-healing polymers with potential applications in various fields. Further studies on the creation of self-healing polymers through catalyst-controlled olefin polymerization are in progress.

ASSOCIATED CONTENT

Supporting Information

The Supporting Information is available free of charge at https://pubs.acs.org/doi/10.1021/acs.macromol.4c00819.

All experimental procedures, methods, NMR spectra, and other characterizations (PDF)
Elasticity of a film of **P2** (Video S1) (MP4)
Self-healing of a film of **P2** (Video S2) (MP4)
Optical microscope video of scratching and self-healing of a film of **P7** (Video S3) (MP4)

AUTHOR INFORMATION

Corresponding Authors

Masayoshi Nishiura − *Advanced Catalysis Research Group, RIKEN Center for Sustainable Resource Science, Wako, Saitama 351-0198, Japan;* orcid.org/0000-0003-2748-9814; Email: nishiura@riken.jp

Zhaomin Hou − *Advanced Catalysis Research Group, RIKEN Center for Sustainable Resource Science, Wako, Saitama 351-0198, Japan; Department of Chemical Science and Engineering, School of Materials and Chemical Technology, Tokyo Institute of Technology, Meguro-ku, Tokyo 152-8552, Japan; Organometallic Chemistry Laboratory, RIKEN Cluster for Pioneering Research, Wako, Saitama 351-0198, Japan;* orcid.org/0000-0003-2841-5120; Email: houz@riken.jp

Authors

Haoran Zhang − *Advanced Catalysis Research Group, RIKEN Center for Sustainable Resource Science, Wako, Saitama 351-0198, Japan; Department of Chemical Science and Engineering, School of Materials and Chemical Technology, Tokyo Institute of Technology, Meguro-ku, Tokyo 152-8552, Japan*

Lin Huang − *Advanced Catalysis Research Group, RIKEN Center for Sustainable Resource Science, Wako, Saitama 351-0198, Japan;* orcid.org/0009-0002-5384-9211

Xia Wu − *Advanced Catalysis Research Group, RIKEN Center for Sustainable Resource Science, Wako, Saitama 351-0198, Japan*

Mingjun Chi − *Advanced Catalysis Research Group, RIKEN Center for Sustainable Resource Science, Wako, Saitama 351-0198, Japan*

Haobing Wang − *Advanced Catalysis Research Group, RIKEN Center for Sustainable Resource Science, Wako, Saitama 351-0198, Japan;* orcid.org/0000-0002-9104-1726

Yuji Higaki − *Department of Integrated Science and Technology, Faculty of Science and Technology, Oita University, Oita 870-1192, Japan;* orcid.org/0000-0002-1032-4661

Tetsuro Murahashi − *Department of Chemical Science and Engineering, School of Materials and Chemical Technology, Tokyo Institute of Technology, Meguro-ku, Tokyo 152-8552, Japan;* orcid.org/0000-0002-2288-0681

Complete contact information is available at: https://pubs.acs.org/10.1021/acs.macromol.4c00819

Author Contributions

#H.Z. and L.H. are contributed equally to this work.

Notes

The authors declare no competing financial interest.

https://doi.org/10.1021/acs.macromol.4c00819
Macromolecules 2024, 57, 7219−7226

■ ACKNOWLEDGMENTS

This work was supported in part by JSPS KAKENHI Grants (JP23H00300 and JP22K05135). We thank Dr. Daishi Inoue (RIKEN Center for Emergent Matter Science) for scanning transmission electron microscopy (STEM) measurement. We are grateful to RIKEN materials characterization team for elemental analyses of copolymers.

■ ABBREVIATIONS

E ethylene
St styrene
AMP 3-(*o*-dimethylaminophenyl)propylene
alt alternating
^{t}BuSt 4-*tert*-butylstyrene
MeSt 4-methylstyrene

■ REFERENCES

(1) Yang, Y.; Urban, M. W. Self-healing polymeric materials. *Chem. Soc. Rev.* **2013**, *42*, 7446−7467.
(2) Patrick, J. F.; Robb, M. J.; Sottos, N. R.; Moore, J. S.; White, S. R. Polymers with autonomous life-cycle control. *Nature* **2016**, *540*, 363−370.
(3) Wang, S.; Urban, M. W. Self-healing polymers. *Nat. Rev. Mater.* **2020**, *5*, 562−583.
(4) Li, B.; Cao, P. F.; Saito, T.; Sokolov, A. P. Intrinsically Self-Healing Polymers: From Mechanistic Insight to Current Challenges. *Chem. Rev.* **2023**, *123*, 701−735.
(5) Urban, M. W.; Davydovich, D.; Yang, Y.; Demir, T.; Zhang, Y.; Casabianca, L. Key-and-lock commodity self-healing copolymers. *Science* **2018**, *362*, 220−225.
(6) Wang, H.; Yang, Y.; Nishiura, M.; Higaki, Y.; Takahara, A.; Hou, Z. Synthesis of Self-Healing Polymers by Scandium-Catalyzed Copolymerization of Ethylene and Anisylpropylenes. *J. Am. Chem. Soc.* **2019**, *141*, 3249−3257.
(7) Yang, Y.; Wang, H.; Huang, L.; Nishiura, M.; Higaki, Y.; Hou, Z. Terpolymerization of Ethylene and Two Different Methoxyaryl-Substituted Propylenes by Scandium Catalyst Makes Tough and Fast Self-Healing Elastomers. *Angew. Chem., Int. Ed.* **2021**, *60*, 26192−26198.
(8) Wang, H.; Yang, Y.; Nishiura, M.; Hong, Y.; Nishiyama, Y.; Higaki, Y.; Hou, Z. Making Polyisoprene Self-Healable through Microstructure Regulation by Rare-Earth Catalysts. *Angew. Chem., Int. Ed.* **2022**, *61*, No. e202210023.
(9) Zhao, Y.; Yin, R.; Wu, H.; Wang, Z.; Zhai, Y.; Kim, K.; Do, C.; Matyjaszewski, K.; Bockstaller, M. R. Sequence-Enhanced Self-Healing in "Lock-and-Key" Copolymers. *ACS Macro Lett.* **2023**, *12*, 475−480.
(10) Lai, H.; Jin, C.; Park, J.; Ikura, R.; Takashima, Y.; Ouchi, M. A Transformable and Bulky Methacrylate Monomer That Enables the Synthesis of an MMA-nBA Alternating Copolymer: Sequence-Dependent Self-Healing Properties. *Angew. Chem., Int. Ed.* **2023**, *62*, No. e202218597.
(11) Gaikwad, S.; Urban, M. W. Ring-and-Lock Interactions in Self-Healable Styrenic Copolymers. *J. Am. Chem. Soc.* **2023**, *145*, 9693−9699.
(12) Li, R.; Zhu, X.; Yu, B.; Jia, S.; Li, Y.; Li, H.; Zheng, J.; Iqbal, M. A.; Zhao, Y.; Li, X. Synthesis of Self-Healing Syndiotactic Polyolefins by Rare-Earth Catalysts. *ACS Catal.* **2024**, *14*, 308−317.
(13) Huang, L.; Yang, Y.; Shao, J.; Xiong, G.; Wang, H.; Nishiura, M.; Hou, Z. Synthesis of Tough and Fluorescent Self-Healing Elastomers by Scandium-Catalyzed Terpolymerization of Pyrenylethenylstyrene, Ethylene, and Anisylpropylene. *J. Am. Chem. Soc.* **2024**, *146*, 2718−2727.
(14) Galli, P.; Vecellio, G. Polyolefins: The most promising large-volume materials for the 21st century. *J. Polym. Sci., Part A: Polym. Chem.* **2004**, *42*, 396−415.
(15) Baier, M. C.; Zuideveld, M. A.; Mecking, S. Post-Metallocenes in the Industrial Production of Polyolefins. *Angew. Chem., Int. Ed.* **2014**, *53*, 9722−9744.
(16) Stürzel, M.; Mihan, S.; Mülhaupt, R. From Multisite Polymerization Catalysis to Sustainable Materials and All-Polyolefin Composites. *Chem. Rev.* **2016**, *116*, 1398−1433.
(17) Sauter, D. W.; Taoufik, M.; Boisson, C. Polyolefins, a Success Story. *Polymers* **2017**, *9*, 185.
(18) Chen, Y.; Kushner, A. M.; Williams, A. G.; Guan, Z. Multiphase design of autonomic self-healing thermoplastic elastomers. *Nat. Chem.* **2012**, *4*, 467−472.
(19) Zou, C.; Chen, C. Polar-Functionalized Crosslinkable, Self-Healing, and Photoresponsive Polyolefins. *Angew. Chem., Int. Ed.* **2020**, *59*, 395−402.
(20) Na, Y.; Chen, C. Catechol-Functionalized Polyolefins. *Angew. Chem., Int. Ed.* **2020**, *59*, 7953−7959.
(21) Nishiura, M.; Hou, Z. Novel polymerization catalysts and hydride clusters from rare-earth metal dialkyls. *Nat. Chem.* **2010**, *2*, 257−268.
(22) Nishiura, M.; Guo, F.; Hou, Z. Half-Sandwich Rare-Earth-Catalyzed Olefin Polymerization, Carbometalation, and Hydroarylation. *Acc. Chem. Res.* **2015**, *48*, 2209−2220.
(23) Yang, Y.; Nishiura, M.; Wang, H.; Hou, Z. Metal-catalyzed C-H activation for polymer synthesis and functionalization. *Coord. Chem. Rev.* **2018**, *376*, 506−532.
(24) Wang, C.; Luo, G.; Nishiura, M.; Song, G.; Yamamoto, A.; Luo, Y.; Hou, Z. Heteroatom-assisted olefin polymerization by rare-earth metal catalysts. *Sci. Adv.* **2017**, *3*, No. e1701011.
(25) Wang, H.; Zhao, Y.; Nishiura, M.; Yang, Y.; Luo, G.; Luo, Y.; Hou, Z. Scandium-Catalyzed Regio- and Stereoselective Cyclopolymerization of Functionalized α,ω-Dienes and Copolymerization with Ethylene. *J. Am. Chem. Soc.* **2019**, *141*, 12624−12633.
(26) Wang, H.; Wu, X.; Yang, Y.; Nishiura, M.; Hou, Z. Co-syndiospecific Alternating Copolymerization of Functionalized Propylenes and Styrene by Rare-Earth Catalysts. *Angew. Chem., Int. Ed.* **2020**, *59*, 7173−7177.
(27) Froidevaux, V.; Negrell, C.; Caillol, S.; Pascault, J. P.; Boutevin, B. Biobased Amines: From Synthesis to Polymers; Present and Future. *Chem. Rev.* **2016**, *116*, 14181−14224.
(28) Pang, B.; Yu, Y.; Zhang, W. Thermoresponsive Polymers Based on Tertiary Amine Moieties. *Macromol. Rapid Commun.* **2021**, *42*, 2100504.
(29) Luo, Y.; Baldamus, J.; Hou, Z. Scandium Half-Metallocene-Catalyzed Syndiospecific Styrene Polymerization and Styrene−Ethylene Copolymerization: Unprecedented Incorporation of Syndiotactic Styrene−Styrene Sequences in Styrene−Ethylene Copolymers. *J. Am. Chem. Soc.* **2004**, *126*, 13910−13911.
(30) It should be noted that 3-(*meta*-dimethylaminophenyl) propylene and 3-(*para*-dimethylaminophenyl)propylene showed no polymerization activity under the same conditions. The formation of an appropriate chelate through the coordination of both the nitrogen atom and the C = C double bond of **AMP** to the catalyst metal is essential for the present copolymerization (See refs 6, 7, 13, 24−26 for related studies).
(31) SeeScheme S1 in the Supporting Information for possible mechanism of **E-AMP** copolymerization.
(32) To avoid the formation of homopolyethylene and **E−AMP** or **E−St** copolymer, the polymerization was terminated by addition of MeOH before the full conversion (complete consumption) of **AMP** or styrene.
(33) SeeScheme S2in the Supporting Information for possible mechanism of **E-St-AMP** terpolymerization.
(34) Li, X.; Hou, Z. Scandium-Catalyzed Copolymerization of Ethylene with Dicyclopentadiene and Terpolymerization of Ethylene, Dicyclopentadiene, and Styrene. *Macromolecules* **2005**, *38*, 6767−6769.
(35) Guo, F.; Nishiura, M.; Koshino, H.; Hou, Z. Scandium-Catalyzed Cyclocopolymerization of 1,5-Hexadiene with Styrene and Ethylene: Efficient Synthesis of Cyclopolyolefins Containing

https://doi.org/10.1021/acs.macromol.4c00819
Macromolecules 2024, 57, 7219−7226

Syndiotactic Styrene−Styrene Sequences and Methylene-1,3-cyclopentane Units. *Macromolecules* **2011**, *44*, 6335−6344.
(36) Guo, F.; Nishiura, M.; Koshino, H.; Hou, Z. Cycloterpolymerization of 1,6-Heptadiene with Ethylene and Styrene Catalyzed by a THF-Free Half-Sandwich Scandium Complex. *Macromolecules* **2011**, *44*, 2400−2403.
(37) Li, X.; Wang, X.; Tong, X.; Zhang, H.; Chen, Y.; Liu, Y.; Liu, H.; Wang, X.; Nishiura, M.; He, H.; Lin, Z.; Zhang, S.; Hou, Z. Aluminum Effects in the Syndiospecific Copolymerization of Styrene with Ethylene by Cationic Fluorenyl Scandium Alkyl Catalysts. *Organometallics* **2013**, *32*, 1445−1458.
(38) It was previously found that a *tert*-butyl substituted **E-AP** copolymer exhibited a higher T_g and stronger mechanical properties than those of the unsubstituted analogs (see ref 19).
(39) It was known that the melting point of syndiotactic poly(4-*tert*-butylstyrene) (T_m = 310 °C) is much higher than that of unsubstituted syndiotactic polystyrene (T_m = 273 °C). See: Ishihara, N.; Kuramoto, M.; Uoi, M. Stereospecific polymerization of styrene giving the syndiotactic polymer. *Macromolecules* **1988**, *21*, 3356−3360.

https://doi.org/10.1021/acs.macromol.4c00819
Macromolecules 2024, 57, 7219−7226